

Ni MINERALIZATION AND PGE CHARACTERIZATION IN THE KABANGA AND LUHUMA Ni-Cu SULFIDE DEPOSITS, NORTH WEST TANZANIA

AS Macheyeke^{1,2}

¹Geological Survey of Tanzania, P.O. Box 903, Dodoma, Tanzania

P. O. Box 1696-Dodoma

Earth Science Institute of Shinyanga, P.O. Box 1016, Shinyanga, Tanzania

Email: asmacheyeke@yahoo.com,

ABSTRACT

Nickel mineralization in the Kabanga sulfide ores is found associated with (1) peripheral veins in the country-rock metapelites, (2) contact type massive sulfide mineralization, and (3) disseminated and vein mineralization. This work, apart from giving general highlight of the Ni mineralization (and other associated elements) in the Kabanga and Luhuma, intends to assess the PGE content in both areas. Cores (mafic-ultramafic and metasedimentary rocks as well as ore sections) from both Kabanga and Luhuma areas were sampled, cut, crushed, pulverized and analyzed for both major and trace elements. Results show that all the Iridium Platinum Group Elements (IPGEs) have very low normalized ratios in each rock and gossan samples as compared to the Palladium Platinum Group Elements (PPGEs). This can be explained by a number of contrasting reasons: (1) the effect of compatibility and incompatibility of IPGEs and PPGEs during mantle melting and fractionation, (2) the IPGEs are often associated with chromites as alloys or sulfides in dunites whilst the PPGEs are often associated with the sulfides of Fe, Ni and Cu and are found in norites, gabbros and dunites. Results also show that, in the Luhuma area lithophiles are 1.5 to 3 times more than in the Kabanga area whereas the Chalcophiles are 1.5 to 6 times more in the Kabanga than in the Luhuma. While three of the PPGE (Pt, Pd and Au) have higher concentrations in both Kabanga and Luhuma areas, they are relatively more in Kabanga than in Luhuma. The IPGE and Rh, have negligible concentrations in both areas. TiO_2 versus Fe_2O_3T , Al_2O_3 versus SiO_2 , PGE versus MgO , as well as Cu/Pd have been compared. They all indicate potentiality of the Kabanga over the Luhuma in terms of PGE. Similar positions of ores from both Luhuma and Kabanga on their TiO_2 versus Fe_2O_3T plots indicate that the Luhuma is also potential for Ni-Cu sulfide deposits particularly on drill holes LUH05 and LUH13 where these samples were taken. In other words, if TiO_2 increases then Ni-Cu sulfide increases and hence the potential for Ni-Cu mineralization.

Key words: Tanzania, Kabanga, Luhuma, PGE, Ni-Cu sulfides

INTRODUCTION

Nickel, a siderophile element (Faure 1991) is also hosted in sulfides (e.g. Naldrett, 1998). In the Kabanga Ni-Cu sulfide ores, Ni is found associated with (1) peripheral veins in the country-rock metapelites, (2) contact type massive sulfide mineralization, and (3) disseminated and vein mineralization associated with the layered silicate rocks of

the central zone of the intrusion (Evans 2000, Macheyeke 2011).

The published work so far in the Kabanga ore deposits has highlighted for the possibility of having Platinum group elements (PGE) as well (e.g. Duchesne, 2004) but to date, no details have been given. This work, apart from giving general highlight of the Ni mineralization in the

Kabanga and Luhuma, intends to assess the PGE content in both areas.

The platinum group elements (PGEs) consist of Osmium (Os), Iridium (Ir), Ruthenium (Ru), Rhodium (Rh), Platinum (Pt), Palladium (Pd) and gold (Au). The first three elements are called Ir-group (IPGE) and the other four elements, the Pd-group (PPGE). The IPGE tend to be compatible during mantle melting whereas the PPGE group are incompatible (Rollinson 1993; Peach & Mathez 1996).

The distribution of PGE and most other chalcophile elements in mafic and ultramafic rocks is controlled predominantly by sulfides. Most of the world's PGE are produced from two types of deposits: PGE-dominated deposits, where PGEs are the main product and Ni-Cu sulfide deposits, where PGE are the by-product. Both types of deposits are closely associated with layered intrusions (Pichard *et al.* 1995, Peach & Mathez 1996, Maier *et al.* 1998). Whereas layering is the function of both time and space, it is expected that, wherever economic PGE deposits are found, evidence for layering is important (e.g. Maier *et al.* 1998). Extensive studies however, have revealed that economically important magmatic Ni-Cu-(PGE) sulfide deposits tend to occur in magma conduit systems, rather than in large layered intrusions (Li *et al.* 2001, Maier *et al.* 2001). Several factors affect the Ni, Cu and PGE grades of the sulfides of the magmatic sulfide deposits, the most important of which include: concentration of these elements in the parental silicate magma, degree of sulfide segregation and immiscibility, reaction between the sulfide droplets and new pulses of mafic magma, and fractionation of the sulfide liquids (Song *et al.* 2011).

When sulfide immiscibility and segregation (a result of crustal contamination) occur relatively earlier than the crystallization of

the silicates, the sulfide droplets could be concentrated at the base of the magma chamber to form massive or semi-massive ores. In contrast, if sulfide segregation and silicate crystallization occur at the same time, they would settle down together and form disseminated sulfide ores (Song *et al.* 2011). This study was conceived in order to study the relationship between Ni and PGE in the Kabanga and Luhuma areas both of which are considered to be potential for Ni-sulfide mineralization and not for PGE even though, evidence for magmatic layering is reported particularly in the Kabanga Main (Macheyeki 2011).

Geological setting

The Kabanga Ni-Cu sulfide deposits and the Luhuma prospect (Fig. 1) are located within the Meso-Proterozoic Karagwe-Ankolean tectonic domain (1.6–1.28 Ga) which is part of the Kibaran metasedimentary belt comprising arenites and pelites with subordinate greywakes and carbonates (Grey 1967, Evans *et al.* 2000).

The Karagwe-Ankolean tectonic domain is characterized by basal sequence of conglomerates and sandstones, with some amygdaloidal basaltic rocks, passing into several cycles of arenite and shale (Stockley and Williams 1938, Grey 1967, Klerkx *et al.* 1987, Tack *et al.* 1994). The shales are interbanded with thin siltstones, and also contain significant amounts of Fe-sulfide and graphite as irregular lenses (Evans *et al.* 2000). Details of the geological setting of both areas is given in Evans *et al.* (2000) and Macheyeki (2011).

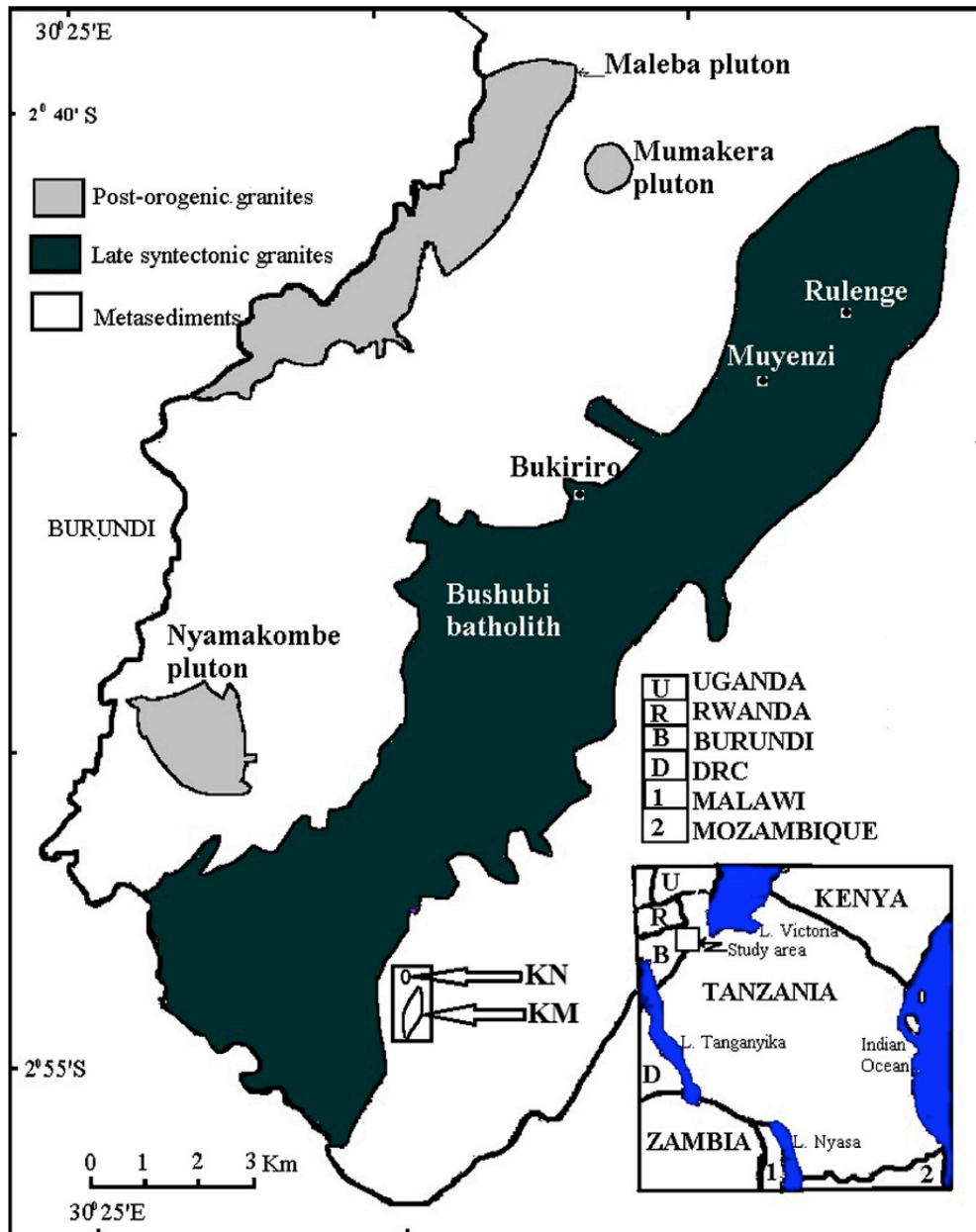


Figure 1: Lithologies of southern domain of Karagwe-Ankolean tectonic domain in relation to the position of the Kabanga area (Ikingura *et al.* (1992)).

Note: KM and KN stand for out lines of Kabanga Main ultramafic body and Kabanga North ultramafic body respectively (Macheyki 2011).

METHODOLOGY

Drill cores from Kabanga North (KN9848 and KN9708) Kabanga Main (KN9873 and KN9869) Ni–Cu sulfide ores sampled (Fig. 2). Three core samples were taken within the massive sulfide based on size of ore zone and frequency of occurrence. Lithologic units (ultramafic/metasedimentary rocks) within hole were also sampled and equally represented. Drill holes LUHD02, LUHD05, LUHD06 and LUHD15 Luhuma prospect were also sampled.

All core samples were cut into two equal halves, washed and dried. One half of every sample was crushed and pulverized using an agate mill, into powder below 75 μ m. Then, pellets weighing between 8 and 10 g each were pressed. For each sample, two pellets

were pressed prior to trace element analysis. Other laboratory routine procedures including preparation of fusion disks in order to homogenize the samples to avoid the problem of matrix effect during major element analysis were followed. The samples were then analyzed for major and trace elements by XRF technique at the University of Stellenbosch. About 50 g of selected pulverized samples were decomposed by Fire-Assay Spectroscopy (AAS) technique, as described in Hall and Bonham-Carter (1988) and Chao and Sanzolone (1992). The sample solutions were then submitted for PGE analysis by ICP–MS at the University of Cape Town. Other details on sample collections, preparations and analysis are given in Macheyeki (2003, 2011).

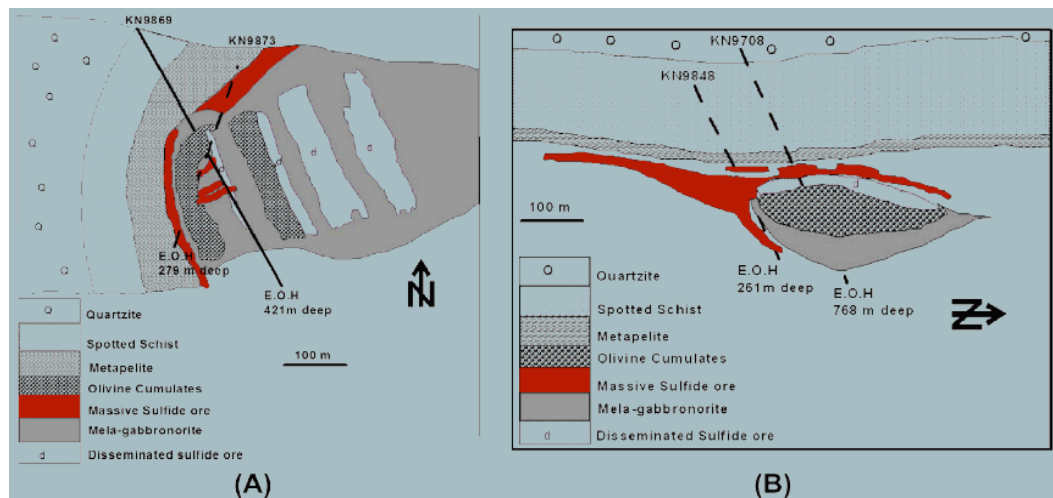


Figure 2 (A) - The sketch of Kabanga Main Ni–Cu sulfide deposit in cross-section and the approximate locations of the drill holes KN9869 and KN9873. (B)-Kabanga North Ni–Cu sulfide deposit in plan-view and the approximate locations of drill holes KN9708 and KN9848.

Note: Olivine cumulates here represent peridotites, whereas mela-gabbro-norite represents pyroxenites and other relatively differentiated mafic–ultramafic rocks (modified after Evans *et al.* 2000, after Macheyeki 2011).

Petrographic studies and mineralization

Detailed petrographic studies as well as mineralization for the Kabanga Ni-Cu sulfide are given in Evans *et al.* (1994, 2000; Macheyeke 2011) and for both the Kabanga and Luhuma by Macheyeke (2011).

**Major and trace elements (selected)
TiO₂ versus Fe₂O₃T in the Kabanga**

The plot of TiO₂ versus Fe₂O₃T for all rock types (including the ore) in the Kabanga area, reveal a graph that is synonymous to an exponential function (Fig. 3). Looking at the graph more closely, one reveals three clusters that are related to (1) unmineralized

metasedimentary rocks on one end of the graph (left), (2) mafic-ultramafic rocks at the middle and (3) the ore on the other end (right). More closer look on this plot also shows that the middle cluster, though representing mafic-ultramafic rocks that are essentially containing disseminated ore, metasedimentary rocks also plot there. The latter are also containing a small quantity of ore. On the right-hand side cluster, massive ore within both metasedimentary and mafic-ultramafic rocks characterize this cluster. Here, the ore refers to massive sulfides of high Ni-Cu grade.

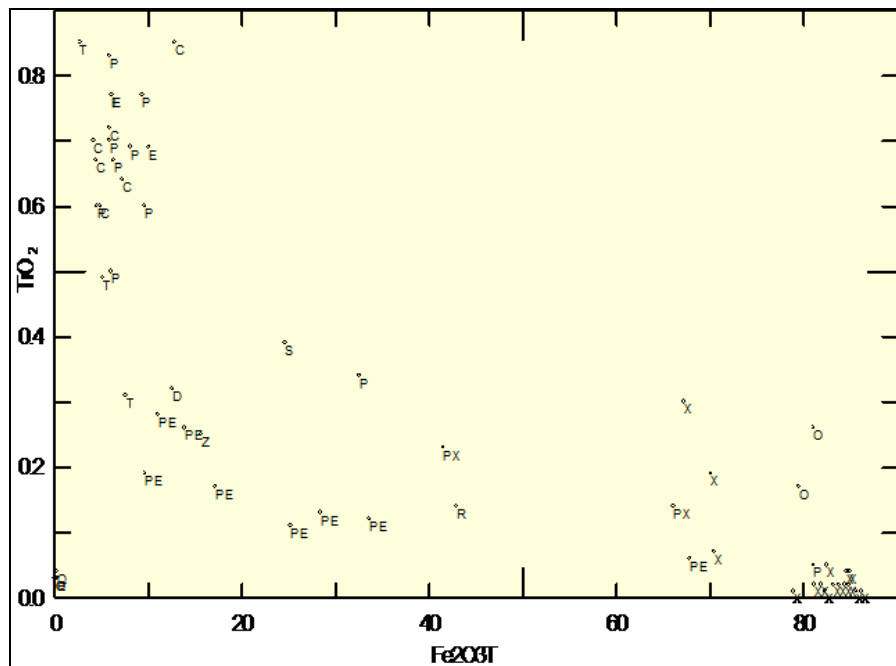


Figure 3. The plot of TiO₂ versus Fe₂O₃T for the Kabanga deposits. The upper right cluster is made up of metasedimentary rocks; middle cluster, mafic and ultramafic rocks and the left cluster represents both disseminated and massive sulfide ores or their products (e.g. gossans). C = Quartz schist, P = metapelites, X = massive sulfide, R = serpentinized rock, T = schist, E = hornfel or metamorphosed fine-grained rock, O = gossan, S = saprolite, Q = quartzite, PX = pyroxenite, PE = peridotite, D = diabase, Z = sheared rock. Note however that P in the middle cluster of the plot is an anomaly.

The massive sulfide ore is defined by Ti ≥ 0 to ≤ 0.1 wt% and Fe₂O₃T = 80- ≈ 87 wt%.

Separating the clusters are two gaps: one is a horizontal gap defined by TiO₂ = 0.4 to ≤

0.5 wt%, $Fe_2O_3T = 3.0$ to ≤ 20 wt%, meaning that the ore is highly oxidized and highly depleted of Titaniferous minerals. The vertical gap is defined by $Ti=0.5$ to 0.35 wt%, $Fe_2O_3T = 50 - \sim 67$ wt%. What would the gaps and the intersection of both gaps ($Ti \approx 0.45$ wt%, $Fe_2O_3T \approx 50$ wt%) define?

samples that plot closer to the origin-they are from a quartzite: the unmineralized Rubona quartzite and (b) we consider all samples together without separating them, because otherwise, each sample type may have its own pattern. It follows therefore that, this graph can be used to predict Ni-Cu sulfide ore position.

These facts and the pattern of the graph however, are only true if (a) we ignore two

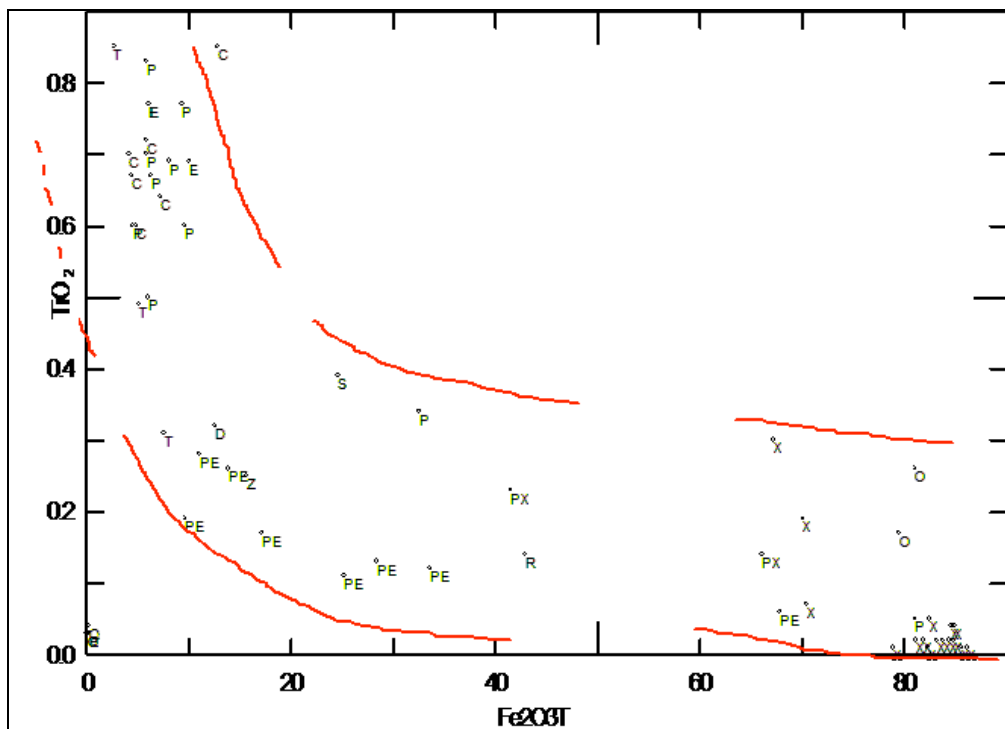


Figure 4 The plot of TiO_2 versus Fe_2O_3T for the Kabanga deposits as in 3. red lines represent approximate trend boundaries. Abbreviations as in Fig. 3.

TiO₂ versus Fe₂O₃T in the Luhuma

The plot of TiO_2 versus Fe_2O_3T for all rock types and the ore in the Luhuma area (Fig. 5) is defined by negative correlation with fairly two clusters: (a) major cluster to the left hand side characterized by mafic-ultramafic rocks and (b) minor cluster characterized by weathered rocks (including

laterites and saprolites) to the right. To the extreme end of the right-hand side, exists a small cluster defined by ore samples of higher values of Fe_2O_3T (up to 80 wt %) same as those from the Kabanga area (See Fig. 4B). These samples are from drill holes LUH05 and LUH06.

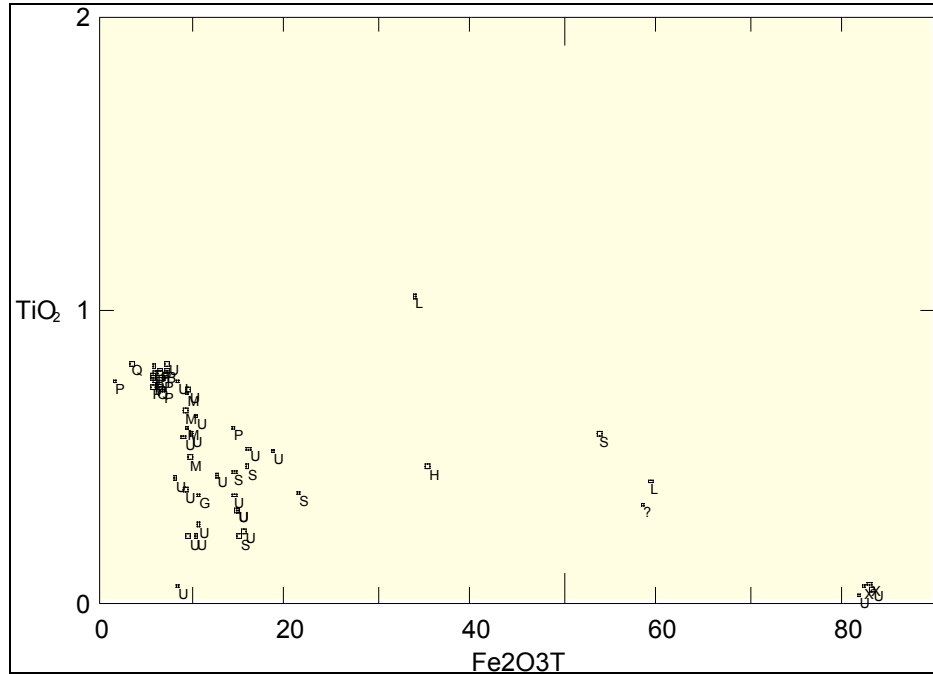


Figure 5: The plot of TiO_2 versus $\text{Fe}_2\text{O}_3\text{T}$ for the Luhuma deposit (s). M = mafic rock, U = ultramafic rock, P = metapelites, G = Gabbro/gabbroic rock, S = saprolite, X = massive sulfide, Q = quartzite? = ultramafic rock?, H = schist?, L = laterite.

Al_2O_3 versus SiO_2 plots

Al_2O_3 versus SiO_2 plots have been used based on the facts that Al_2O_3 is hosted in rocks rich in feldspars, platy minerals such as micas, biotite, sericites and metasedimentary rocks. SiO_2 is hosted in silicates (in this case, mafic-ultramafic rocks) as well as in quartzites.

As for the TiO_2 versus $\text{Fe}_2\text{O}_3\text{T}$, the Al_2O_3 versus SiO_2 plots (Fig. 6A) show three clusters for the Kabanga deposits area: one cluster corresponding to the massive sulfides and disseminated ore in mafic-ultramafic rocks near the origin, mafic-ultramafic rocks and fairly mineralized metasedimentary rocks at the middle and finally unmineralized metasedimentary rocks to the right of the plot (Fig. 6A). The major difference between the Al_2O_3 versus SiO_2 plot is that while the TiO_2 versus $\text{Fe}_2\text{O}_3\text{T}$

plot show a negative correlation (or exponential function), the Al_2O_3 versus SiO_2 plot show positive correlation meaning that generally, Al_2O_3 content increases with decrease in SiO_2 content. However, zooming in the plot, one realizes that the bottom and middle part of the plot obey this argument whereas the right corner cluster (related to unmineralized metasedimentary rocks) behaves differently: it shows negative correlation, meaning that the decrease of Al_2O_3 corresponds with increase of SiO_2 content

For the Luhuma area (Fig. 6B), only two (2) clusters occur (the lower left and the middle part) both of which are related by a positive correlation trend. No metasedimentary data were studied-which probably explains why the negative correlation observed in Fig. 6A is not evidenced in Fig. 6B.

Al₂O₃ plots

The plots Al₂O₃ (Fig. 7) from both Kabanga and Luhuma show different patters: from Kabanga a two populations plot is shown whereas, a one population plot is revealed from the Luhuma. Each population is thought to represent one source of Al₂O₃ or a phase in which Al₂O₃ is hosted. It is thought that the Al₂O₃ is mainly hosted by metasemetary rocks (? mica rich schists). The presence of two populations of Al₂O₃ in

the Kabanga area may also indicate that one population corresponds with Al₂O₃ background values (0 – 9 wt%) corresponding with massive sulfide ore, and another population may represent anomalous values of Al₂O₃ (~ 12.5 – 21.5 wt%) from metasedimentary rocks. The ore population of Al₂O₃ from the Luhuma area imply that Al₂O₃ source is essentially one; i.e. from mafic-ultramafic rocks. No metasedimentary rocks data are included here.

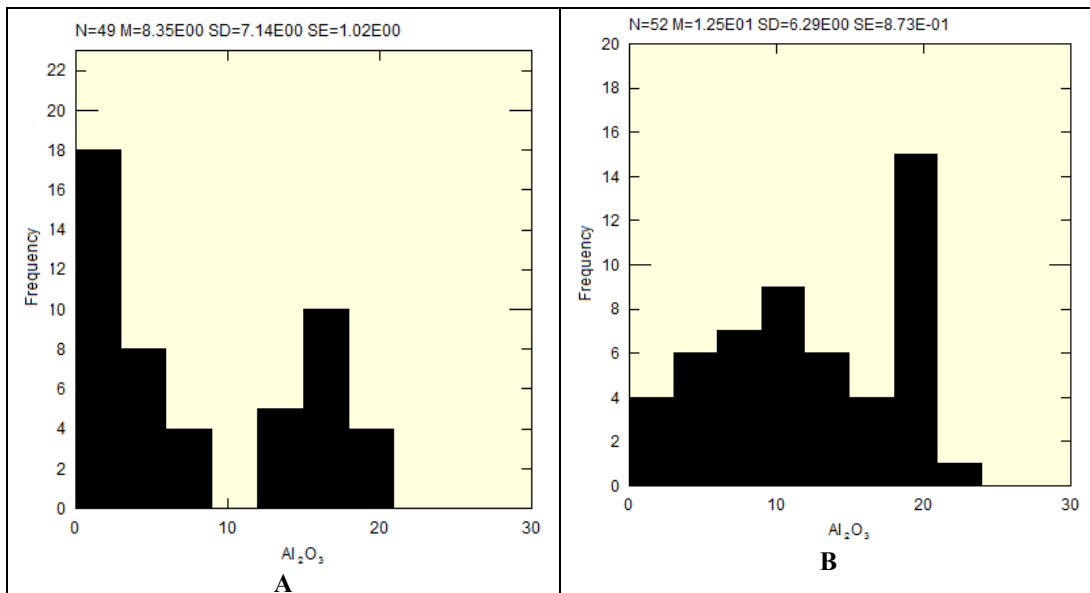
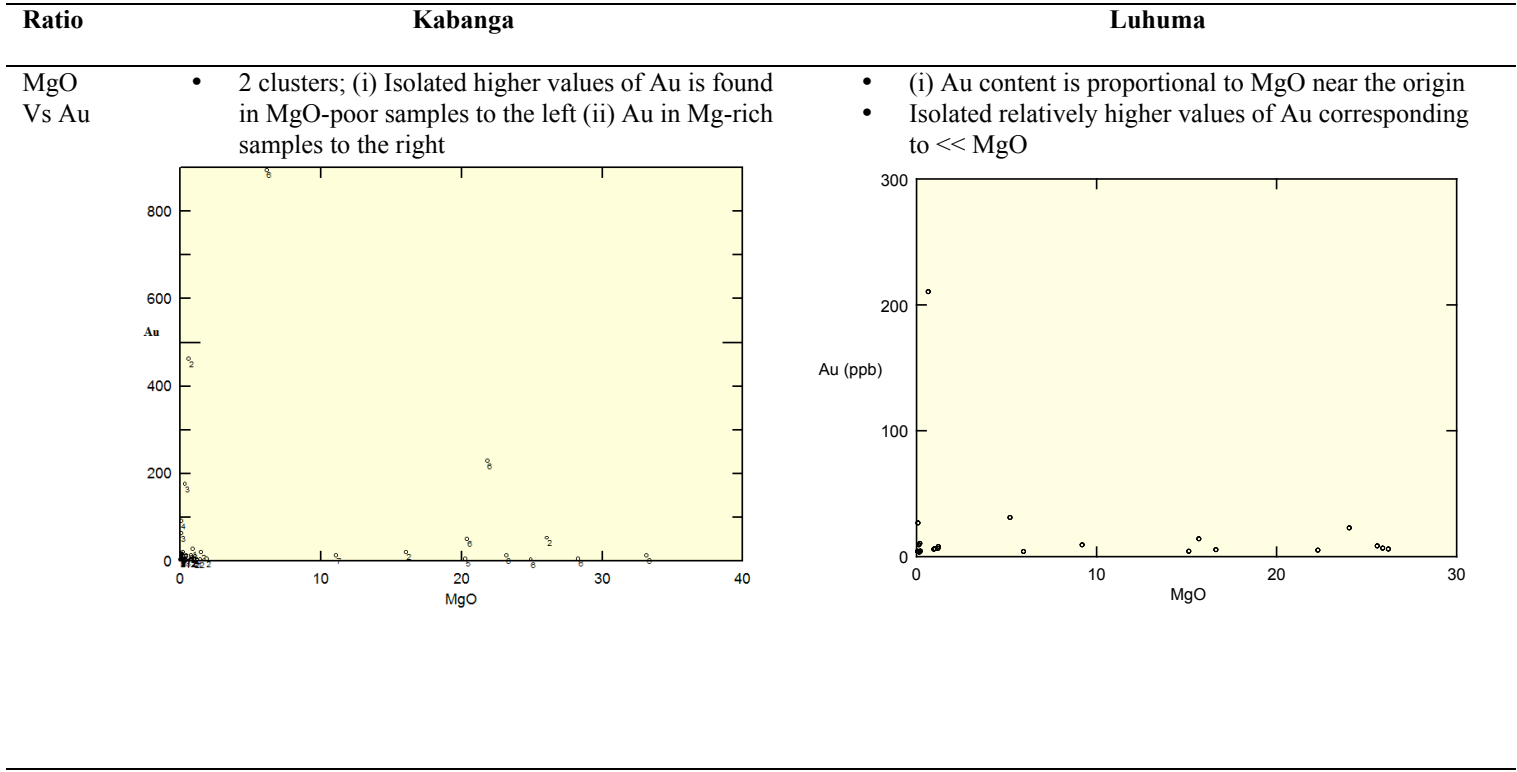


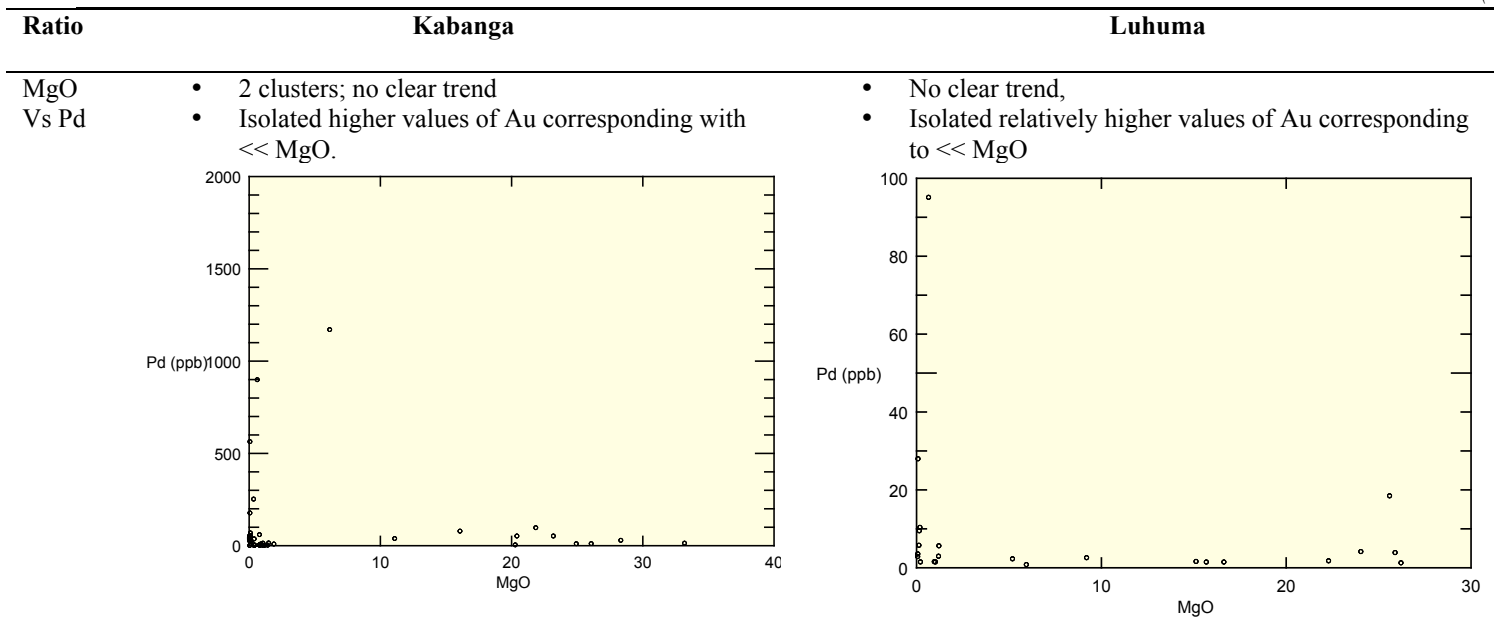
Figure 7: (A) Histograms of Al₂O₃ from Kabanga and (B) Luhuma

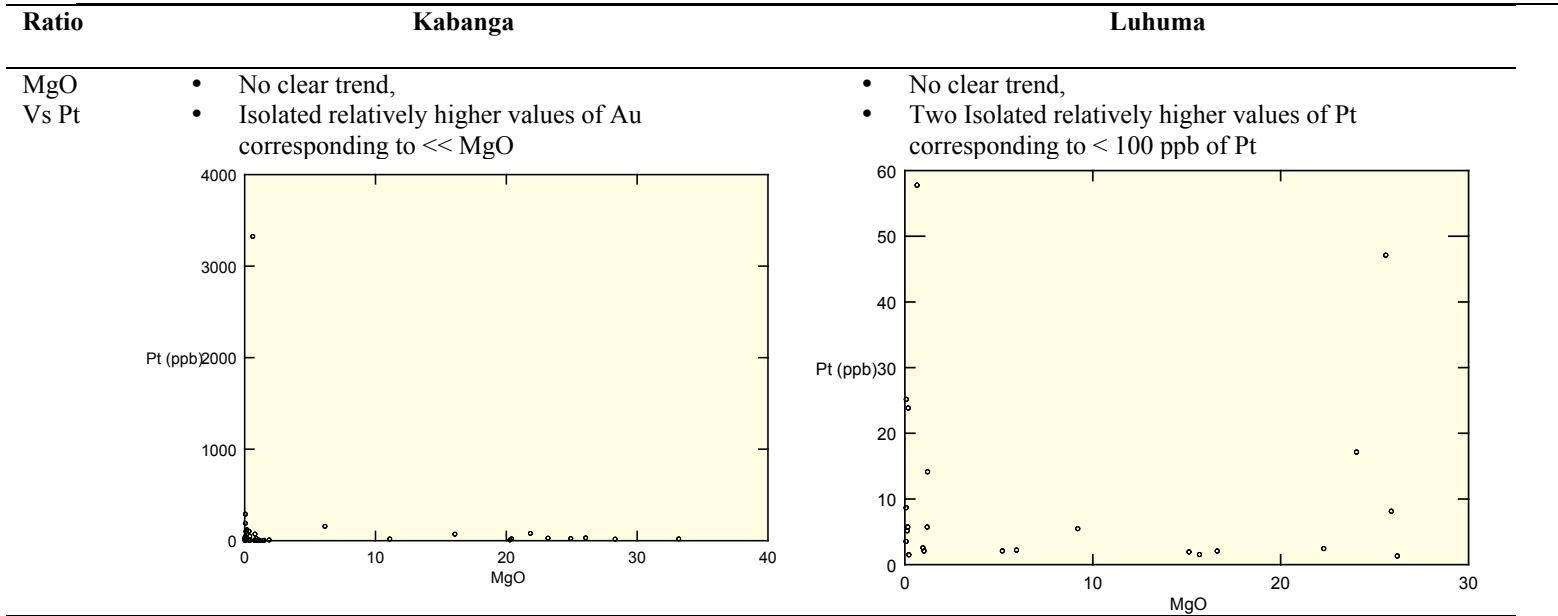
PGE versus MgO

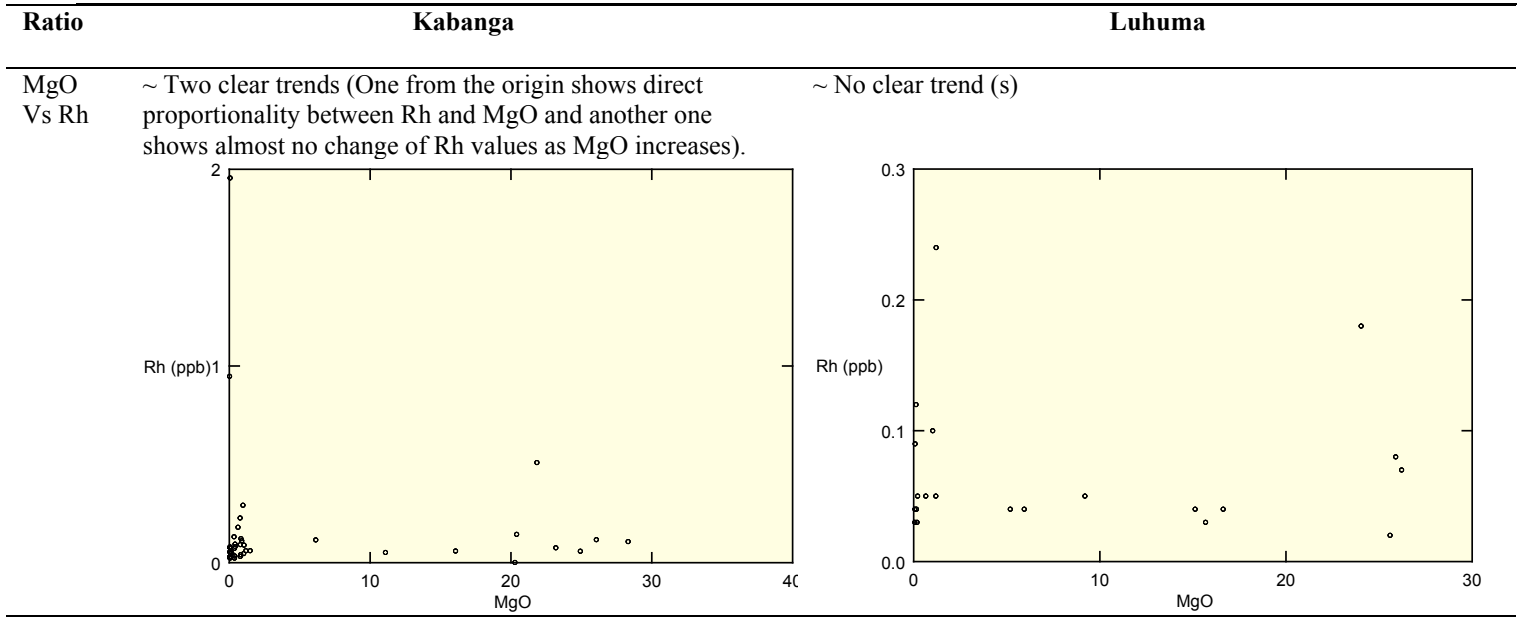
The plots of PGE versus MgO have been presented (Fig. 8). They indicate variable trends; generally, PPGE increases with increasing MgO. The plots of data from PPGE obtained from Kabanga also show clear trends as compared to inconsistent trends of both PPGE and IPPGE from the Luhuma area.

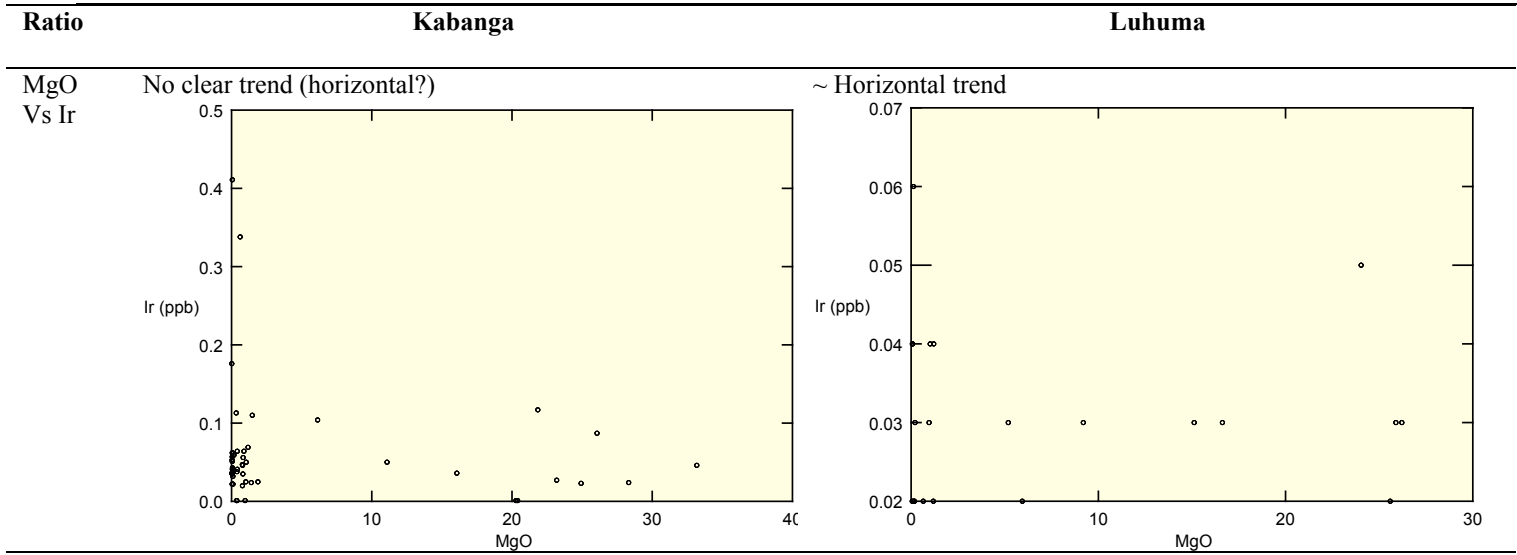
IPGE versus MgO (wt%) plots in the Kabanga show variable trends where Au seems to be associated with MgO poor samples to the left and it is also associated with MgO rich samples to the right. For the Luhuma area, Au is proportional to MgO near the origin (MgO < 1 wt % and Au < 25ppb). From Au > 25 ppb, proportionality does not exist. i.e. there is constant Au content (≈ 25ppb) from MgO = 5 wt% (Fig. 8).

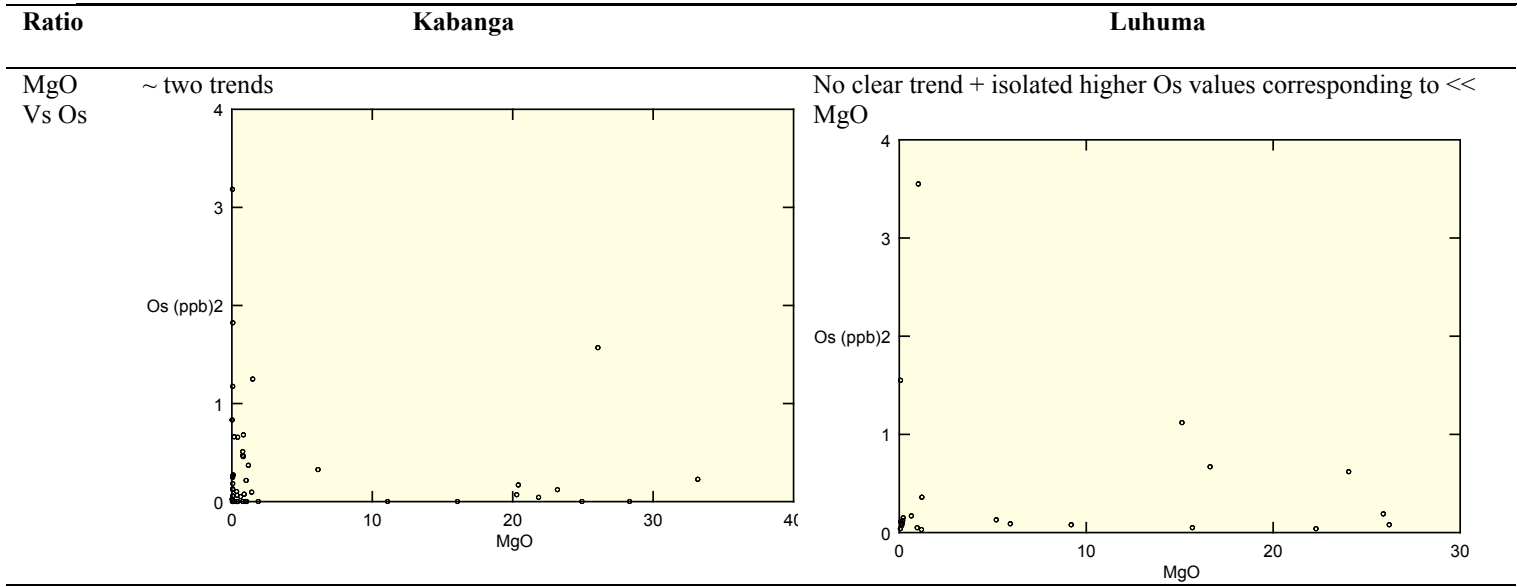


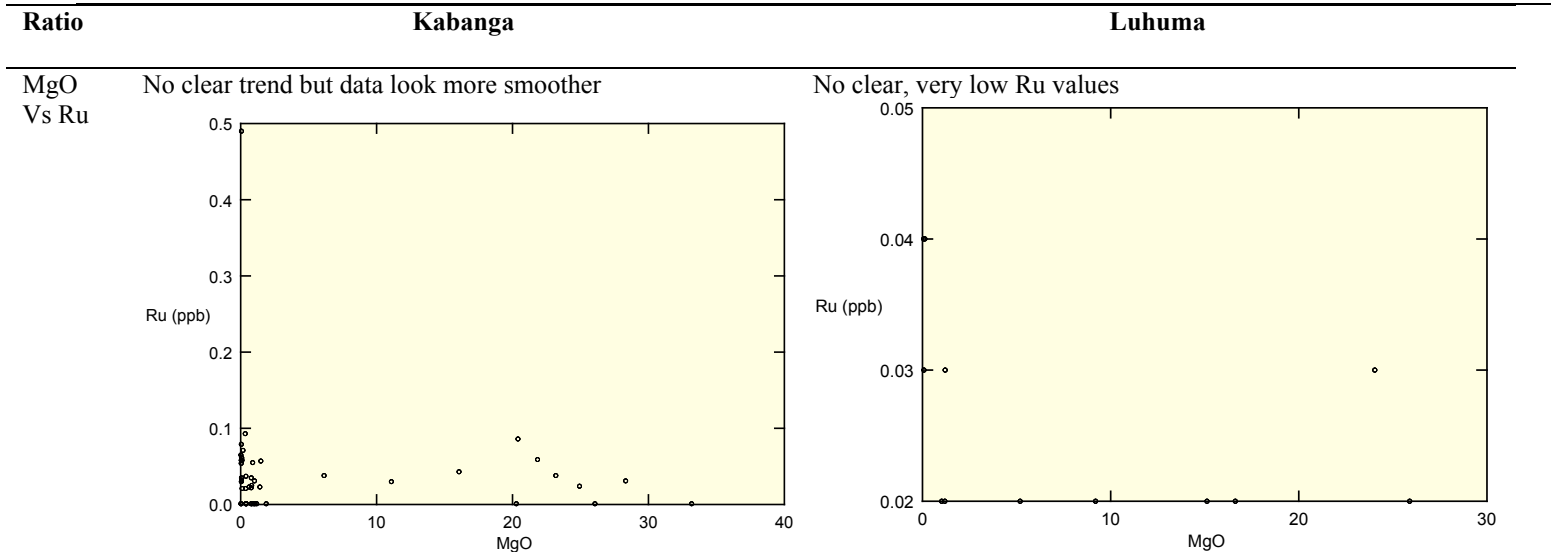












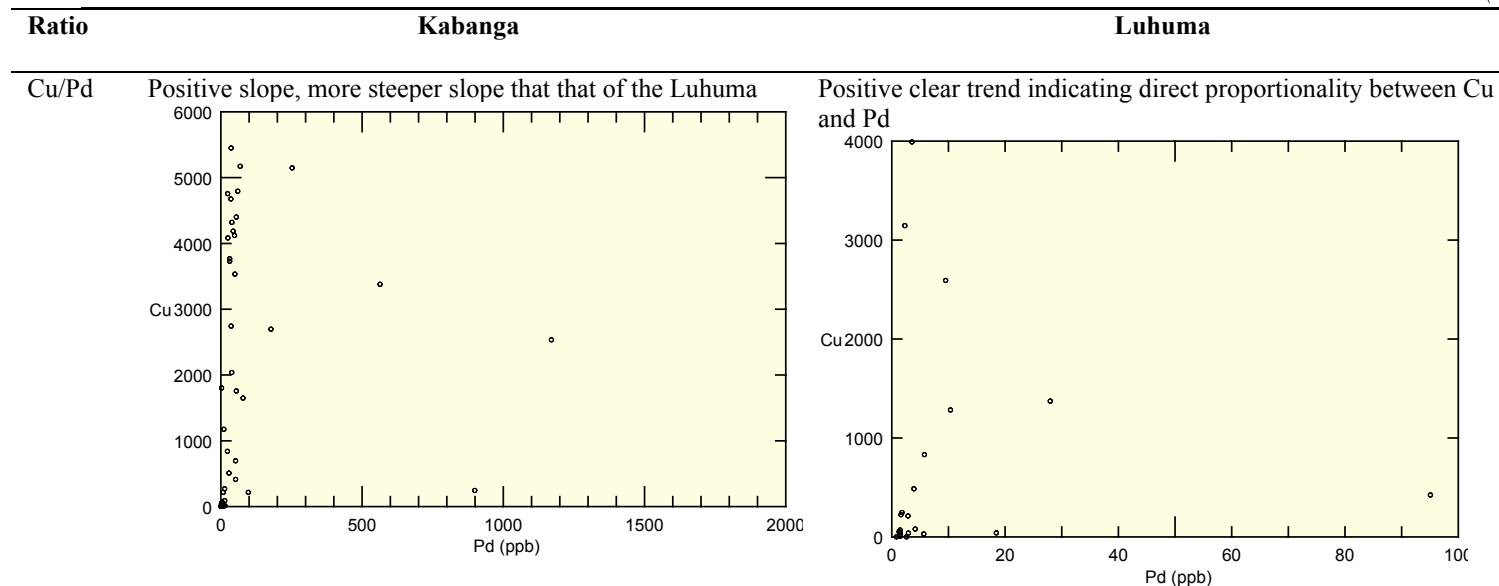


Figure 8: The plots of PGE versus MgO for PGE from the Kabanga and the Luhuma.

Table 1 A Statistical summary of the trace element concentrations in metasedimentary rocks from Kabanga, ultramafic bodies from both Kabanga area (KULTRA) and Luhuma area (LULTRA), Kabanga Main ore (KMORE), Kabanga North ore (KNORE), Luhuma ores (LORE). QTZ and MPEL, stand for quartzite and metapelite respectively. Numbers in brackets are average chemical compositions of ultramafic rocks in *ppm*, except for Au which is in *ppb* from Turekian and Wadepohl (1961) and Vinogradov (1962) in Faure G (1991). * = Calculated from data listed by Herrmann (1970). Chalc = chalcophile, Litho = lithophile, Sidero = Siderophile. S and L (after *) stand for Siderophile and Lithophile respectively. (After Macheyeki 2011).

	QTZ (N=2)	SCHIST (N=8)	MPEL (N=10)	KULTRA (N=8)	LUTRA (N=8)	KMORE (N=9)	KNORE (N=8)	LORE (N=6)	Element type (Faure 1991)
ELEMENT	GEOMEAN	GEOMEAN	GEOMEAN	GEOMEAN	GEOMEAN	GEOMEAN	GEOMEAN	GEOMEAN	
Cr (ppm)	257	142	171	2496 (1800)	1978 (1800)	907	1108	947	Chalc* S
Mo (ppm)	1	1	2	4 (0.3)	2 (0.3)	17	18	10	Chalc* L
Nb (ppm)		11	10	2 (9)	3 (9)		2	2	Litho
Zr (ppm)	33	261	254	22 (38)	43 (38)	21	19	22	Litho
Y (ppm)	0	24	24	6 (-)	12 (-)	6	4	5	Litho
Sr (ppm)		70	83	18 (5.5)	33 (5.5)	11		26	Litho
U (ppm)		3	3	4 (0.002)	(0.002)				Litho
Rb (ppm)	2	140	90	8 (1.1)	25 (1.1)	9	7	15	Litho
Th (ppm)	0	15	16	4 (0.0045)	5 (0.0045)				Litho
Pb (ppm)		22	39	54 (0.5)	9 (0.5)	14	32	31	Chalc
Ga (ppm)		21	20	7 (1.8)	9 (1.8)	9	13	8	Chalc* L
Zn (ppm)		47	98	101 (40)	71 (40)	161	177	103	Chalc
Cu (ppm)		24	108	310 (15)	68 (15)	3519	4117	1113	Chalc
Ni (ppm)	631	93	1132	5208 (2000)	562 (2000)	23934	24490	4300	Sidero
Nd (ppm)		22	30	(1.9*)	21 (1.9*)				Chalc

V (ppm)	5	97	71	114 (40)	165 (40)	37	44	83	Litho
Ce (ppm)	6	54	66	12 (3.5*)	18 (3.5*)	11	10	12	Litho
La (ppm)	1	30	36	9 (1.3*)	12 (1.3*)	11		9	Litho
Ba (ppm)	18	578	351	42 (0.7)	86 (0.7)	27	16	60	Litho
Ru (ppb)		0	0	0	0	0	0	0	Sidero
Rh (ppb)	0	0	0	0	0	0	0	0	Sidero
Pd (ppb)	1	3	11	44	3	49	53	11	Sidero
Os (ppb)		0	0	0	0	0	0	0	Sidero
Ir (ppb)	0	0	0	0	0	0	0	0	Sidero
Pt (ppb)	1	4	8	33	5	36	42	13	Sidero
Au (ppb)	3	7	8	32 (60)	7 (60)	10	15	13	Sidero

Table 1 B Ratios between the element concentrations in both areas. OR = average crustal concentration of ultramafic rocks. KB=Kabanga, LH = Luhuma. N= Number of data used. Other abbreviations are the same as in Table 1A. (After Macheyeke, 2011).

	QTZ (N=2)	SCHIST (N=8)	MPEL (N=10)	KULTRA (N=8)	OR	KULTRA/ OR	LUTRA (N=8)	LULTRA/ OR	KB/LUH	LH/ KB	KMORE (N=8)	KNORE (N=8)	LORE (N=6)	Element type (Faure, 1991)
Cr (ppm)	257	142	171	2496	1800	1.39	1978	1.10	1.26	0.79	907	1108	947	Chalc*S
Mo (ppm)	1	1	2	4	0.3	13.33	2	6.67	2.00	0.50	17	18	10	Chalc*L
Nb (ppm)		11	10	2	9	0.22	3	0.33	0.67	1.50		2	2	Litho
Zr (ppm)	33	261	254	22	38	0.58	43	1.13	0.51	1.95	21	19	22	Litho
Y (ppm)	0	24	24	6			12				6	4	5	Litho
Sr (ppm)		70	83	18	5.5	3.27	33	6.00	0.55	1.83	11		26	Litho
U (ppm)		3	3	4	0.002	2000.00	0.002	1.00	2000.00	0.00				Litho
Rb (ppm)	2	140	90	8	1.1	7.27	25	22.73	0.32	3.13	9	7	15	Litho
Th (ppm)	0	15	16	4	0.0045	888.89	5	1111.11	0.80	1.25				Litho
Pb (ppm)		22	39	54	0.5	108.00	9	18.00	6.00	0.17	14	32	31	Chalc
Ga (ppm)		21	20	7	1.8	3.89	9	5.00	0.78	1.29	9	13	8	Chalc*L
Zn (ppm)		47	98	101	40	2.53	71	1.78	1.42	0.70	161	177	103	Chalc
Cu (ppm)		24	108	310	15	20.67	68	4.53	4.56	0.22	3519	4117	1113	Chalc
Ni (ppm)	631	93	1132	5208	2000	2.60	562	0.28	9.27	0.11	23934	24490	4300	Sidero
Nd (ppm)		22	30		1.9	0.00	21	11.05	0.00					Chalc

Macheyeki - Ni Mineralization and PGE Characterization ...

	QTZ (N=2)	SCHIST (N=8)	MPEL (N=10)	KULTRA (N=8)	OR	KULTRA/ OR	LUTRA (N=8)	LULTRA/ OR	KB/LUH	LH/ KB	KMORE (N=8)	KNORE (N=8)	LORE (N=6)	Element type (Faure, 1991)
V (ppm)	5	97	71	114	40	2.85	165	4.13	0.69	1.45	37	44	83	Litho
Ce (ppm)	6	54	66	12	3.5	3.43	18	5.14	0.67	1.50	11	10	12	Litho
La (ppm)	1	30	36	9	1.3	6.92	12	9.23	0.75	1.33	11		9	Litho
Ba (ppm)	18	578	351	42	0.7	60.00	86	122.86	0.49	2.05	27	16	60	Litho
Ru (ppb)		0	0	0			0				0	0	0	Sidero
Rh (ppb)	0	0	0	0			0				0	0	0	Sidero
Pd (ppb)	1	3	11	44			3				49	53	11	Sidero
Os (ppb)		0	0	0			0				0	0	0	Sidero
Ir (ppb)	0	0	0	0			0				0	0	0	Sidero
Pt (ppb)	1	4	8	33			5				36	42	13	Sidero
Au (ppb)	3	7	8	32	60	0.53	7	0.12	4.57	0.22	10	15	13	Sidero

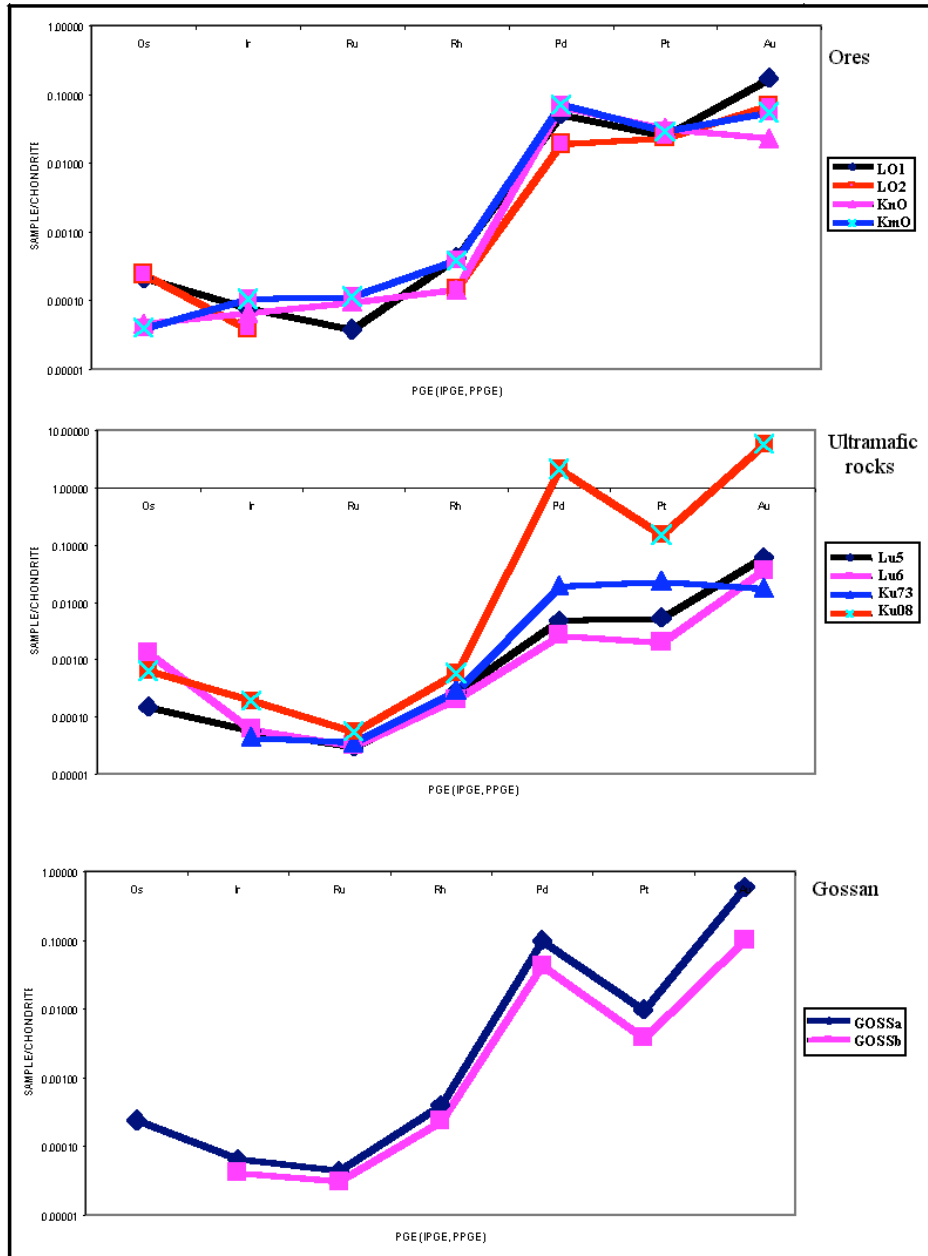


Figure9: Chondrite-normalized PGE (IPGE, PPGE) plot for the Kabanga ores (knO and kmO), Luhuma ores (Lo1 and Lo2), Kabanga ultramafic bodies (ku73 and ku08), Luhuma ultramafic bodies (Lu5 and Lu6) and gossans from Kabanga main (GOSSa and GOSSb). The order of the elements (left to right) is of decreasing melting point. Chondrite values used are from Naldrett and Duke (1980) and Rollinson (1993).

Cu/Pd plots

Plots of Cu/Pd are presented. They show positive correlation (with some few outliers) for the Kabanga area and positive clear correlation for the Luhuma. The slopes are ≈ 30 for the Kabanga and 150 for the Luhuma (Fig. 8). The difference between the two slopes implies that Cu than Pd are enriched differently in Kabanga and Luhuma.

Chondrite normalized plots of PGE

Chondrite normalized plots have been presented firstly in a summary statistical table (Table 1) and also as chondrite normalized plots (Fig. 9).

Fig. 9 shows that all the IPGEs have very low normalized ratios in each rock and in gossan samples as compared to the PPGEs. This can be explained by a number of contrasting reasons. (1) the effect of compatibility and incompatibility of IPGEs and PPGEs during mantle melting and fractionation, (2) the IPGEs are often associated with chromites as alloys or sulfides in dunites whilst the PPGEs are often associated with the sulfides of Fe, Ni and Cu and are found in norites, gabbros and dunites (Rollinson 1993). Palladium indeed shows positive anomalies as compared to Pt. According to Rollinson (1993), the ultramafic and mafic rocks do show positive Pd and negative Pt and Au anomalies.

Again, all plots for ultramafic rocks and ores from Luhuma areas are relatively subdued as compared to those from Kabanga. These differences in contrasts of the plots could be attributed to controls by major element composition of the magma (Pichard *et al.* 1995), which acts on the variations of sulfidesulfide capacity in residual liquids. Important major elements are $\text{CaO} + \text{Al}_2\text{O}_3$ and SiO_2 . The FeO activity has also been pointed as an important element contributing to the variation mentioned above.

Other trace elements

Table 1A, B show that, lithophiles are 1.5 to 3 times more concentrated in Luhuma than in Kabanga. This observation however excludes U that seems to be highly concentrated in Kabanga to the order of 2000 times the average crustal concentration of U in ultramafic rocks (Faure 1991). Chalcophiles are more concentrated in Kabanga than in Luhuma at orders of 1.5 to 6 times. Elements that are concentrated in more than one phase are of the order of 1 to 2 times higher in Kabanga than in Luhuma. These include Cr, Mo and Ga.

Platinum: the average concentration of Pt in the Luhuma ultramafic rocks is the same as that in metasedimentary rocks in Kabanga (i.e. 1-8 ppb). In massive sulfides (ore) however, the values rise slightly (mean, 13ppb). Contrarily, Pt values in ultramafic rocks from Kabanga are 5 times more higher than those in Luhuma, and in Luhuma ores, Pt values are 3 time less than those in Kabanga ores.

DISCUSSION

The fact that IPGE versus MgO (wt%) plots show unclear trends whereas PPGE (except Pt) show clear trends in the Kabanga area reflects the degree of compatibility of the IPGE and incompatibility of the PPGE in the upper mantle. Data from Fig. 10 show that Pt has been abnormally concentrated in metasedimentary rocks particularly on the western part of the Kabanga main deposit (as intersected by drill hole KN9869)-hence its unique trends with silicates or MgO (wt%).

It can also be shown that the silicate magma from Kabanga have two major sources of Al_2O_3 (wt%) as a plot of Al_2O_3 (wt%) from Kabanga shows two populations, probably reflecting Al_2O_3 (wt%) from silicate and country rocks or one population reflects of Al_2O_3 background values and the other,

anomalous values. For the Luhuma, such a plot show only one population, this probably

indicate that the Al_2O_3 (wt%) used here comes from one major source; the silicates.

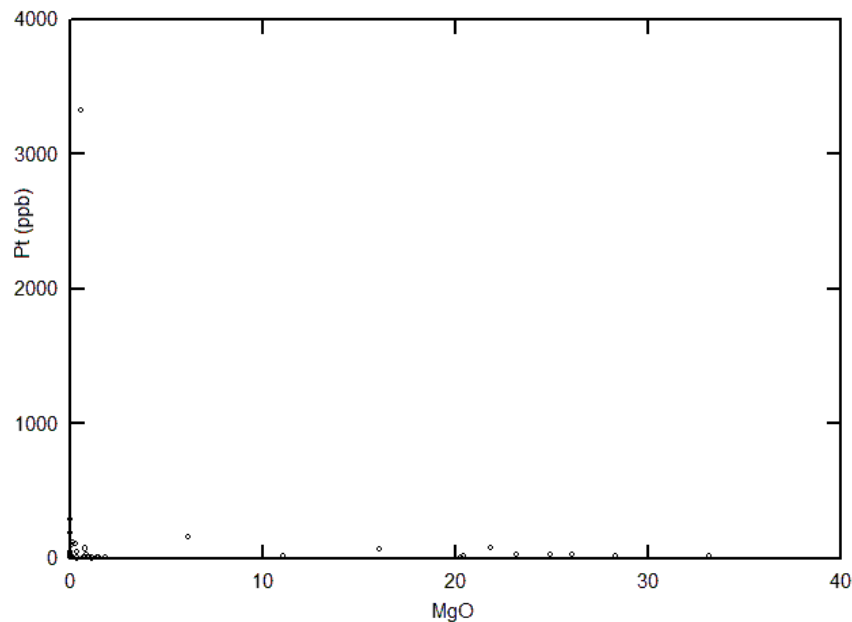


Figure 10 The plot of Pt (ppb) versus MgO (wt %) for the Kabanga Ni-Cu sulfide deposit. Isolated higher values of Pt (up to > 3000 ppb i.e. > 3%) in the Kabanga Main ore body were intersected.

NiO (wt%) versus MgO (wt%) plots show that there is a positive correlation in the Luhuma and a negative correlation in the Kabanga. However, this fact is true for NiO (wt%) ≥ 2 (Figs. 11) and mineralized zones are characterized by MgO (wt%) of ≤ 2 meaning that relatively low values of Ni concentration are proportional to silicate concentrations but as Ni values increase above a certain level, the relationship is different.

TiO_2 versus $\text{Fe}_2\text{O}_3\text{T}$, Al_2O_3 versus SiO_2 , PGE versus MgO , PGE versus Cr as well as Cu/Pd have been compared.

A unique picture, worthy mentioning, is the one that is revealed when $\text{Fe}_2\text{O}_3\text{T}$ and TiO_2 are plotted. The picture is clearer for the data from Kabanga than those from Luhuma:

clusters and gaps (horizontal and vertical) are defined. From these results one may attempt to say that the values of TiO_2 close to 0.45 wt% and the values of $\text{Fe}_2\text{O}_3\text{T} \approx 50$ wt%, when obtained from exploration activities are not characteristic of any samples from Kabanga (Fig. 4). They respectively separate barren metasedimentary rocks-disseminated sulfide ore and massive sulfide ore-disseminated sulfide ore.

PGE versus MgO indicate variable trends; generally increasing with increase in MgO . For Cu/Pd, the plots show positive correlation from both Kabanga and Luhuma ores implying that Cu than Pd are enriched differently in Kabanga and Luhuma. Steeper slope in the Luhuma than in the Kabanga may also imply higher Cu values in Luhuma

than in the Kabanga. However, the fact that PGE increase with increase in MgO means that PGE (and hence Pd) are higher in the MgO higher area (the Kabanga area) and

that the Cu/Pd higher slopes in the Luhuma means that Pd is depleted or is present in relatively small amount as compared to Kabanga (the MgO-rich area).

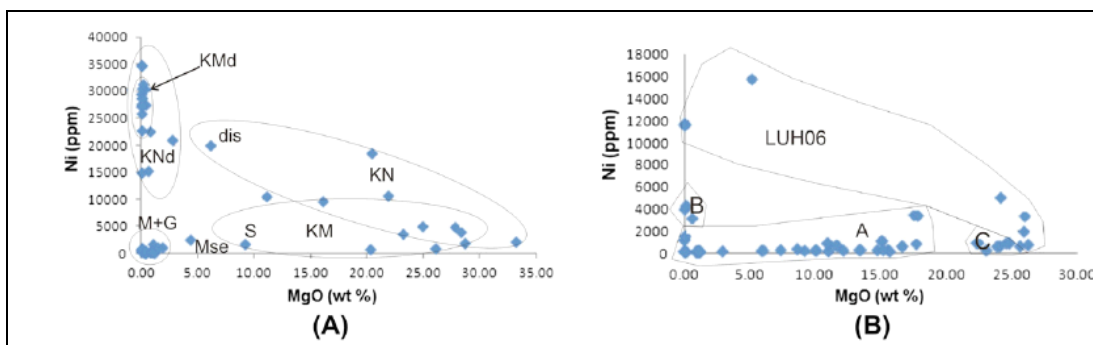


Figure 11: (A) MgO (wt.%) versus Ni (ppm) for the Kabanga area. KM = Kabanga Main, KN = Kabanga North, S = suprolite, dis = disseminated ore, KMd = detached ore from Kabanga Main, KNd = detached ore from Kabanga North. M + G = metapelite and gossan. (B) MgO (wt.%) versus Ni (ppm) for the Luhuma area. 'A' represents fields of drill holes LUH02, 05, 06, 13 and 15; 'B' represent fields of drill holes LUH02, 05, 13 and 15; and 'C' represent fields of drill holes LUH05, 06, 13 & 15. LUH06, is the exclusively the field of LUH06 (For location see Fig. 12); (From Macheyeki 2011).

All these results indicate potentiality of the Kabanga over the Luhuma in terms of PGE. However, similar positions of ores from both Luhuma and Kabanga on their TiO_2 versus Fe_2O_3/T plots indicate that the Luhuma is also potential for Ni-Cu sulfide deposits particularly on drill holes LUH05 and LUH13 where these samples were taken from. In Macheyeki (2011), the areas in which these drill holes are located were recommended as suitable drill targets for Ni-Cu sulfide deposits (Fig. 12). What could this imply? This could be compared to the facts reported by Song *et al.* (2011) that several factors that lead to concentration of Ni are therefore not only limited to presence of Ni in parental magma but also depend on; (i) crustal contamination and assimilation of sedimentary sulfides; e.g. Naldrett, 1998), (ii) degree of sulfide segregation and immiscibility, (iii) reaction between sulfide droplets and new pulses of mafic magmas as well as fractionation of sulfide liquids. Recent studies have, however, shown that

the genesis of orthomagmatic deposits is controlled by magma chamber processes such as fractional crystallization (with or without contamination, Duchesne *et al.* 2004), immiscibility and magma mixing.

In Table 1A, B, the results cast some light on the degree of silicate-sulfide interaction in the two areas (deposits). The possible explanation would be that the silicate rocks in Kabanga have segregated more (as a results of silicate rocks-metasedimentary rocks interaction (Naldrett 1998) or that relatively more pulses of chalcophile rich silicate magma have been pumped in the Kabanga area than in the Luhuma area.

While three of the PPGE (Pt, Pd and Au) have significant concentrations in both Kabanga and Luhuma areas, there are relatively more in Kabanga than in Luhuma. The IPGE and Rh, have negligible concentrations in both areas.

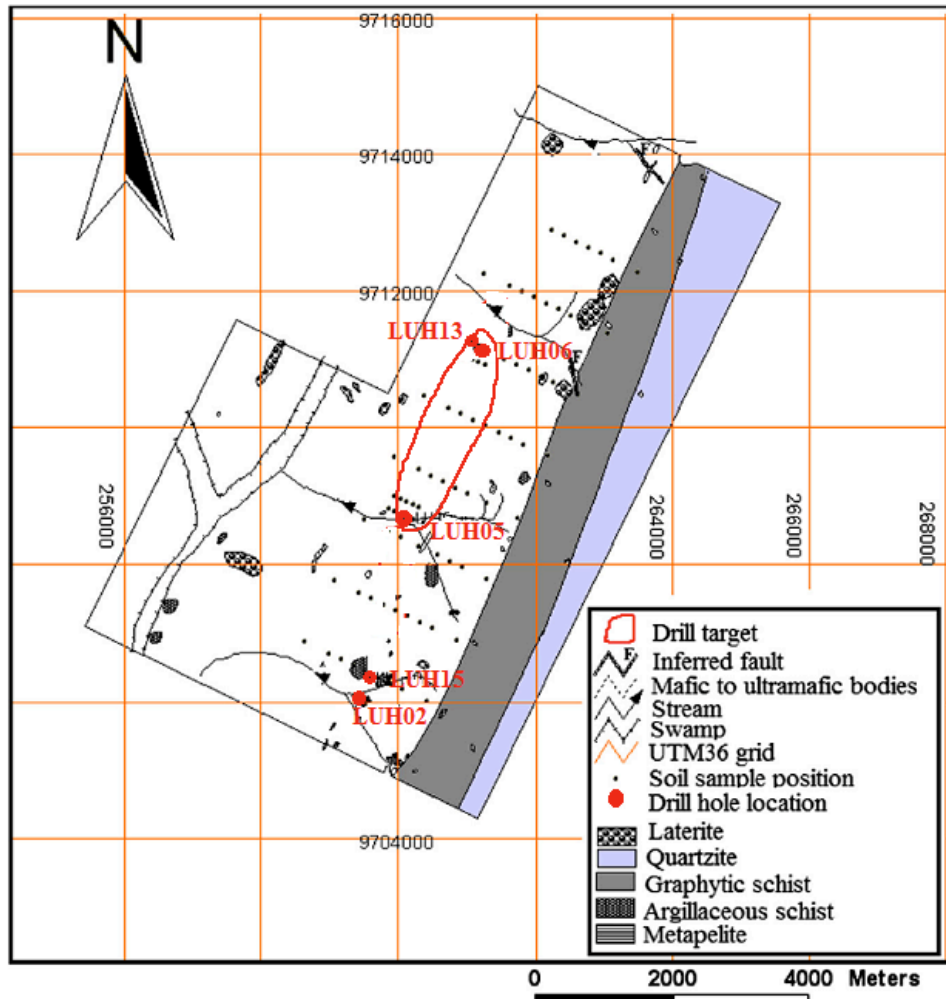


Figure 12: The overlay of the proposed drill targets on the geology of the Luhuma prospect. The relatively most potential area is within the area defined by coordinates UTM36 259799E/9707413N (From Macheyeke 2011).

CONCLUSION AND RECOMMENDATIONS

It has been shown that PGE (especially PPGE) have higher concentrations in the Kabanga than in the Luhuma. IPPGE have insignificant values in either part. The Kabanga area, particularly the Kabanga Main need be studied for PPGE in detail. In

terms of Ni-Cu sulfide deposits, the Luhuma area need not be ruled out even though its PGE contents are too low to justify for PGE exploration. The zone between LUH05 and LUH13 is likely to be the most potential for Ni-Cu sulfide deposit (s), Fig. 12.

ACKNOWLEDGEMENT

Large part of this work was funded by Anglo American (T) Ltd. Thanks to Prof. C. Okujeni from the University of the Western Cape, RSA for his guidance during the entire research. I am also indebted to Dr. S. Many from the University of Dar Es Salaam who read and commented on the manuscript.

REFERENCES

- Chao TT, Sanzolone RF 1990 Decomposition techniques, *J. Geochem. Explor.* **44**: 65-106.
- Duchesne, JC, Liégeois JP, Deblond A, Tack L, 2004 Petrogenesis of the Kabanga-Musongati layered mafic-ultramafic intrusions in Burundi (Kibaran Belt): Geochemical, Sr-Nd isotopic constraints and Cr-Ni behavior. *J. Afr. Earth Sci.* **39**: 133-145.
- Evans, D, Boad I, Byemelwa L, Gilligan J, Kabete J, Marcet P, Sanga M 1994 Intrusion of the Kabanga Magmatic Ni Deposits, Tanzania-Morphology and Geochemistry, Dar-Es-Salaam. BHP Mineral International Exploration Inc., Internal Report.
- Evans DM, Boad I, Byemelwa L, Gilligan J, Kabete J, Marcet P 2000 Kabanga magmatic nickel sulfide deposits, Tanzania: morphology and geochemistry of associated intrusions. *J. Afr. Earth Sci.* **30** (3): 651–674.
- Faure G, 1991 Principles and applications of Geochemistry. 2d ed. Prentice-Hall, Inc. Upper Sanddle River, New Jersey 07458, USA.
- Grey IM 1967 (Compiler). Quarter Degree Sheet 29 and 29W, Ngara Geological Map with Explanation 1:125,000, Tanzania, Mineral Resources Dodoma.
- Hall GEM, Bonham-Carter 1988. Review of methods to determine gold, platinum and palladium in production-oriented geochemical laboratories, with application of statistical procedure to test bias. *J. Geochem. Explor.* **30**: 255-286.
- Ikingura JR, Reynolds PH, Watkinson DH, Bell K 1992 $^{40}\text{Ar}/^{39}\text{Ar}$ dating of granites of NE Kibaran Belt (Karagwe-Ankolean), northwestern Tanzania. *J. Afr. Earth Sci.* **15** (3/4): 501-511.
- Klerkx J, Liégeois JP, Laveau J, Claessens W 1987 Crustal evolution of the northern Kibaran Belt, Eastern and Central Africa. In: Kroner, A. (Ed.), *Proterozoic Lithospheric Evolution*. American Geophysical Union, Washington, 217-233.
- Li CS, Naldrett AJ, Ripley EM, 2001 Critical factors for the formation of a nickel-copper deposit in an evolved magma system: lessons from a comparison of the Pants Lake and Voisey's Bay sulfide occurrences in Labrador, Canada. *Mineralium Deposita* **36** (1): 85e92.
- Macheyeki AS 2003 *Lithogeochemical Vectors Associated with the Kabanga Ni-Cu Sulfide Deposits, NW Tanzania*: M.Sc. thesis, Cape Town, The University of the Western Cape, 117p.
- Macheyeki AS 2011 Application of lithogeochemistry to exploration for Ni–Cu sulfide deposits in the Kabanga area, NW Tanzania. *J. Afr. Earth Sci.* **61**: 62-81.
- Maier WD, Barnes SJ, De Waal SA 1998 Exploration for Magmatic Ni-Cu-PGE Sulfide Deposits: A review of recent advances in the use of Lithogeochemical tools and their application in some South African ores. *South Afr. J. Geol.* **101** (3): 237-253.
- Maier WD, Li CS, De Waal SA 2001 Why are there no major Ni-Cu sulfide deposits in large layered mafic-ultramafic intrusions? *The Canadian Mineralogist* **39** (2): 547e556.
- Maier WD 2005. Platinum-group element (PGE) deposits and occurrences: Mineralization styles, genetic concepts, and exploration criteria. *J. Afr. Earth Sci.*, **41**: 165-191.

- Naldrett A.J., Duke J.M., 1980. Platinum metals in magmatic sulfide ores. *Science*, 208: 1417-1424.
- Naldrett AJ 1998 World class Ni-Cu-PGE deposits: key factors in their genesis. *Mineralium deposita* **34**: 227-240.
- Peach CL, Mathez EA 1996 Constraints on the formation of Platinum-Group Element Deposits in Igneous Rocks. *Econ. Geol.* **91**: 439-450.
- Pichard C., Amossé J, Piboule M, Giovenazzo D, 1995 Physical and Chemical Constraints on Platinum-Group Element Behavior during Crystallization of a Basaltic Komatiite Liquid: Examples of the Proterozoic Delta Sill, New Quebec, Canada. *Econ. Geol.* **90**: 2287-2303.
- Rollinson H 1993 Using geochemical data: evaluation, presentation, interpretation. United Kingdom: Longman Group Ltd. (Geochemical series) 150-170.
- Song, X *et al.* 2011 Magmatic Ni-Cu-(PGE) deposits in magma plumbing systems: Features, formation and exploration, *Geoscience Frontiers*, doi:10.1016/j.gsf.2011.05.005
- Stockley GM. Williams GJ 1938. Explanation of the geology, Degree Sheet 1, Karagwe Tin-fields. Tanganyika Territory Department of Lands and Mines Bulletin, Geological Division: Dar Es Salaam, 10, 91.
- Tack L, Liégeois JP, Deblond A, Duchesne, JC 1994 Kibaran A-type granitoids and mafic rocks generated by two mantle sources in a late orogenic setting (Burundi). *Precamb. Res.* **68**: 323-356.